Honeybee flight dynamics and pair separation in windy conditions

Bardia Hejazi[1,2,*], **Hugo Antigny**[1,3], **Sophia Huellstrunk**[1,4], **Eberhard Bodenschatz**[1,2,5,6,*]

[1] Laboratory for Fluid Physics, Pattern Formation and Biocomplexity, Max Planck Institute for Dynamics and Self-Organization (MPI-DS), 37077 Göttingen, Germany
[2] Max Planck University of Twente Center for Complex Fluid Dynamics, MPI-DS, 37077 Göttingen, Germany
[3] Universite Grenoble Alpes, Grenoble INP - Phelma, Grenoble 38000, France
[4] Princeton University, NJ 08544, United States
[5] Institute for Dynamics of Complex Systems, University of Göttingen, 37077 Göttingen, Germany
[6] Laboratory of Atomic and Solid State Physics and Sibley School of Mechanical and Aerospace Engineering, Cornell University, 14853 Ithaca, NY, USA
[*] Author to whom any correspondence should be addressed.

E-mail: `bardia.hejazi@ds.mpg.de, eberhard.bodenschatz@ds.mpg.de`

Abstract.
Animals and living organisms are continuously adapting to changes in their environment. How do animals, especially those that are critical to their ecosystem, respond to rapidly changing conditions in their environment? Here, we report on the three-dimensional trajectories and orientations of flying honeybees under calm and windy conditions in front of the hive entrance. We find that the average speeds, accelerations and angular velocities of honeybees increase with increasing wind speeds. We observed that pair separation between honeybees is highly controlled and independent of wind speeds. Our results on the coordination used by honeybees may have potential applications for swarm intelligent manned and unmanned aerial vehicles.

Keywords: Honeybee, Insect, Flight control, Collective behavior

1. Introduction

Animal behavior is influenced by the surrounding environment and changes to the environment. The change in air currents and surface winds impacts the behavior of flying animals, and with the potential increase in wind speeds (Zeng et al., 2019) due to climate change, flying animals may need to adapt their behavior to new conditions. Flying insects such as honeybees manage changes in surrounding air flows (Crall et al., 2017) quite well and maintain flight control even under strongly turbulent conditions (Hejazi

et al., 2022). In this work we further explore how honeybees behave and fly in extreme conditions to better understand the mechanisms utilized by honeybees especially when flying in close proximity to one another. The ability for insects to maintain stability and control while in flight (Sun, 2014) and understanding the strategies they use, can aid in improving the swarm intelligent systems required for the navigation of small-scale flying robotic collectives (Srinivasan, 2011; Farrell Helbling and Wood, 2018).

Insects are particularly well suited for research because of their small size, abundance, and the relative ease in which experiments can be carried out on them. Which is why fruit flies have been a long favored example of flying insects for studies (Harrington, 2014; Vogel, 1966; Fuller et al., 2014; Ortega-Jiménez and Combes, 2018). Insects also provide us with the exceptional opportunity to study swarm intelligence, i.e., their group and social dynamics, as demonstrated by studies of swarming midges (Attanasi et al., 2014; Feng and Ouellette, 2023). Another insect of particular interest is the honeybee (and other species of bees), due to their important ecological role as natural pollinators (Hung et al., 2018; Delaplane et al., 2000) on the one hand, but also due to their unique social structure. Experiments studying the social behavior and dynamics of honeybees mostly focus on activity at the hive entrance (Butler and Free, 1952; Magnier et al., 2018; Ngo et al., 2019; Chiron et al., 2013; Babic et al., 2016). Studies that investigate swarms look at stationary collectives that are not in flight, such as work investigating the mechanical stability of honeybee swarms (Shishkov et al., 2022; Peleg et al., 2018).

Experiments studying honeybee flight are usually carried out in the laboratory and investigate the flight of individuals, focusing on wing aerodynamics (Ahmed et al., 2022; Altshuler et al., 2005) and dynamical responses to different air flows (Crall et al., 2017; Jakobi et al., 2018). Although not as numerous as laboratory studies, field experiments have also investigated honeybee flight stability in windy conditions and observe that honeybees increase roll stability by extending their hind legs (Combes and Dudley, 2009). More recently, experiments have studied honeybee flight dynamics outside and looking at the trajectories of honeybees near the hive entrance (Mahadeeswara and Srinivasan, 2018), while also considering the influence of turbulence on honeybee flight (Hejazi et al., 2022). However, there is still a lack of research on the collective flight of honeybees and how they avoid collisions with one another mid-flight. Studies suggest that collision avoidance is achieved through visual sensing (Groening et al., 2012). Honeybees may also use other senses for navigation and collision avoidance, for instance, it has been shown that honeybees are capable of sensing electric fields (Greggers et al., 2013; Sutton et al., 2016) and use this to their advantage when foraging (Clarke et al., 2013) while also contributing to atmospheric electric fields when swarming (Hunting et al., 2022). In this study we examine the flight dynamics and pair statistics of honeybees near the hive entrance, outside in their natural environment. We track honeybees using high-speed, high-resolution cameras and investigate their flight and behavior in natural calm weather conditions and compare to conditions where we generate winds with different mean flow velocities.

2. Methods

The experiments were performed at the Max Planck institute for Dynamics and Self-Organization (MPI-DS) in Göttingen, Germany. Experiments were performed on July 27, 2022, from 10:00 am to 16:00 pm. The weather during the experiments was calm with minimal natural air flow and no precipitation. The ambient temperature during the experiments was between 20-23 degrees Celsius. Experiments were performed at the entrance of a honeybee hive from the *Apis mellifera carnica* species, as shown in Fig. 1. Performing experiments in front of the entrance allows us to study landing and take-off dynamics and to additionally examine the interactions between pairs of honeybees mid-flight.

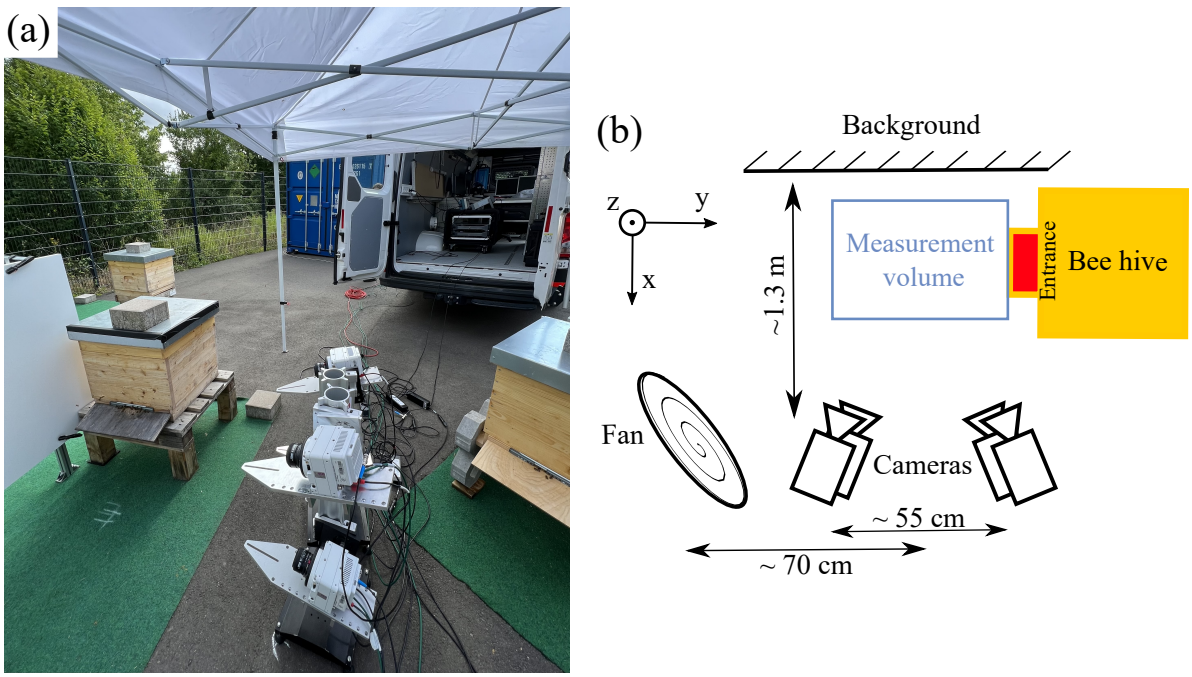

Figure 1. (a) Experimental setup showing the honeybee hive, cameras and background with the overhead shade from the pavilion to protect the cameras from the elements. Also shown is the mobile laboratory where data servers are located and experimentalists monitor recordings. (b) Schematic of the experimental setup showing the location and distances between cameras, background, and fan. The measurement volume in our experiments is approximately 60 (L) x 70 (W) x 30 (H) centimeters where the length is along $\hat{y}$, the width along $\hat{x}$, and the height along $\hat{z}$.

We created wind in front of the hive using an industrial grade ventilation fan that has three speed settings. The vector perpendicular to the plane of the fan was approximately at a 45° angle with respect to $-\hat{x}$ and $\hat{y}$ with a slight upwards tilt in the $\hat{z}$ direction. We measured the wind speed produced by the fan using a testo 405i thermal anemometer probe. The thermal anemometer was also used to determine wind direction and speed for when the fan was off. We measured air flow velocities by placing the probe

in the center of the measurement volume before each experiment and removing it before recording videos. We performed experiments under three different wind conditions; no wind, moderate wind, and strong wind. The details of the experimental conditions and wind velocities are given in Table 1. The natural air flows were approximately 9% of the moderate and 5% of the strong wind settings of the fan. Thus, the natural air flow was much weaker than the flow produced by the fan.

Table 1. Air flow speed measurements along with the number of video recordings for each experiment setting. The mean flow velocity in the x, y, and z direction is reported, with the total mean flow velocity being U.

Exp.	U_x (m/s)	U_y (m/s)	U_z (m/s)	U (m/s)	No. recordings
No wind	-0.2	0.1	0.05	0.23	25
Moderate wind	-1.0	2.2	0.5	2.46	25
Strong wind	-1.9	4.0	0.6	4.46	10

We recorded images using 4 Phantom VEO4K 990L cameras equipped with 50 mm lenses capturing 4096 $\times$ 2034 pixel images at 200 frames per second with approximately 30 seconds of continuous image capture before the camera RAM was full and data transfer was initiated. We recorded a total of 25 videos for the no wind and moderate wind conditions and recorded 10 videos for the strong wind conditions. We recorded less videos for strong wind conditions to limit the time we exposed the honeybees to intense winds and to minimize disturbance to the hive. The cameras had different viewing angles which created an effective measurement volume of 60 (L) x 70 (W) x 30 (H) centimeters. Cameras are triggered and synced using an external signal generator. We used a small pavilion that covered the cameras to protect them from overheating due to direct exposure to the sun and potential harm from any precipitation that may occur during experimentation. We use two data servers for rapid data transfer of video recordings from the camera RAM. The data servers were mounted on a shockproof rack located in a mobile laboratory. The mobile laboratory is a custom van meant for experiments in the field. The experimentalists were seated in the van while experiments were underway and monitored the image capture and download.

Imaging and tracking of honeybees is based on previous methods and in-house codes used to track honeybees using consumer-grade GoPro cameras (Hejazi et al., 2022) and similar high-speed Phantom cameras used to track particles in turbulence experiments (Hejazi et al., 2019; Hejazi, 2021). An example image from one camera is shown in Fig. 2 with a zoomed in panel showing a honeybee. The high-resolution cameras used in these experiments allowed us to clearly image honeybees and all their features. We were also able to determine honeybee body orientations using a nonlinear fitting algorithm. The routine optimizes for the honeybee position and orientation by minimizing the difference between a model that is projected onto the camera image plane and the actual honeybee images (Hejazi et al., 2019).

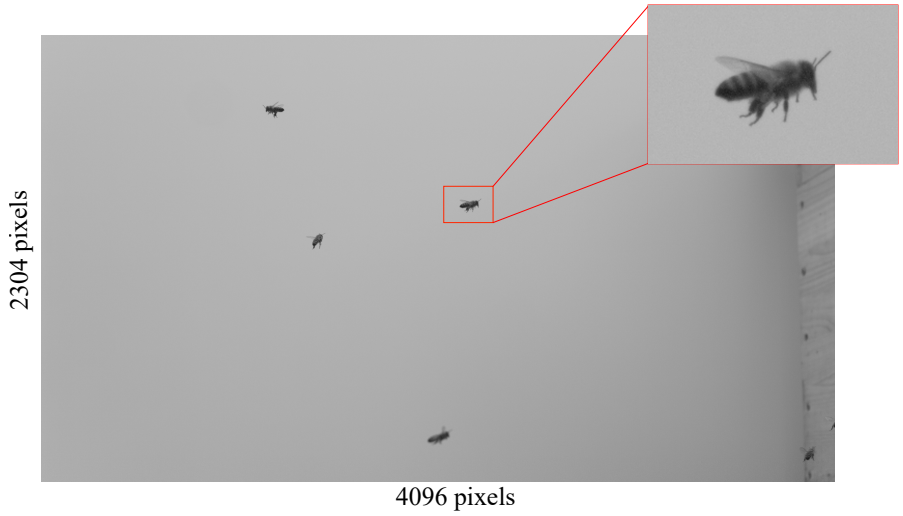

Figure 2. An example image from one camera and a zoomed in view of a honeybee demonstrating the image quality and our ability to finely resolve honeybee features.

3. Results

We calculated honeybee flight velocities and accelerations using polynomial fits to the three-dimensional (3D) trajectories. We only used data in the analysis where the stereomatching error was no more than 5 pixels. The resulting average tracking error across all cameras was approximately one pixel. Furthermore, we only analyzed tracks longer than 10 frames. Table 2 shows the total number of tracks, mean track length, and maximum track length of each wind condition experiment. We can see that as the wind intensity increases the mean and maximum track lengths decreases, thus honeybees seem to not linger in windy conditions when compared to mild, no wind conditions.

Table 2. The total number of tracks, mean track length, and maximum track length for each experiment setting.

Exp.	No. tracks	Mean track length	Max. track length
No wind	3894	59	504
Moderate wind	3948	43	459
Strong wind	797	37	272

Figure 3 shows the probability distribution function (PDF) of the honeybee velocity and acceleration components in different wind conditions. From Fig. 3 (a,c,e) we can clearly see a directional preference in the velocity components. Here when there is no wind generated by the fan (blue filled circles), the honeybee has larger velocities when leaving the hive as shown by the skewed PDF of v_y towards larger negative values. While under these conditions, there is no preferential direction to v_x and v_z. However, as we introduced wind, the velocity component PDF's changed in that the honeybee

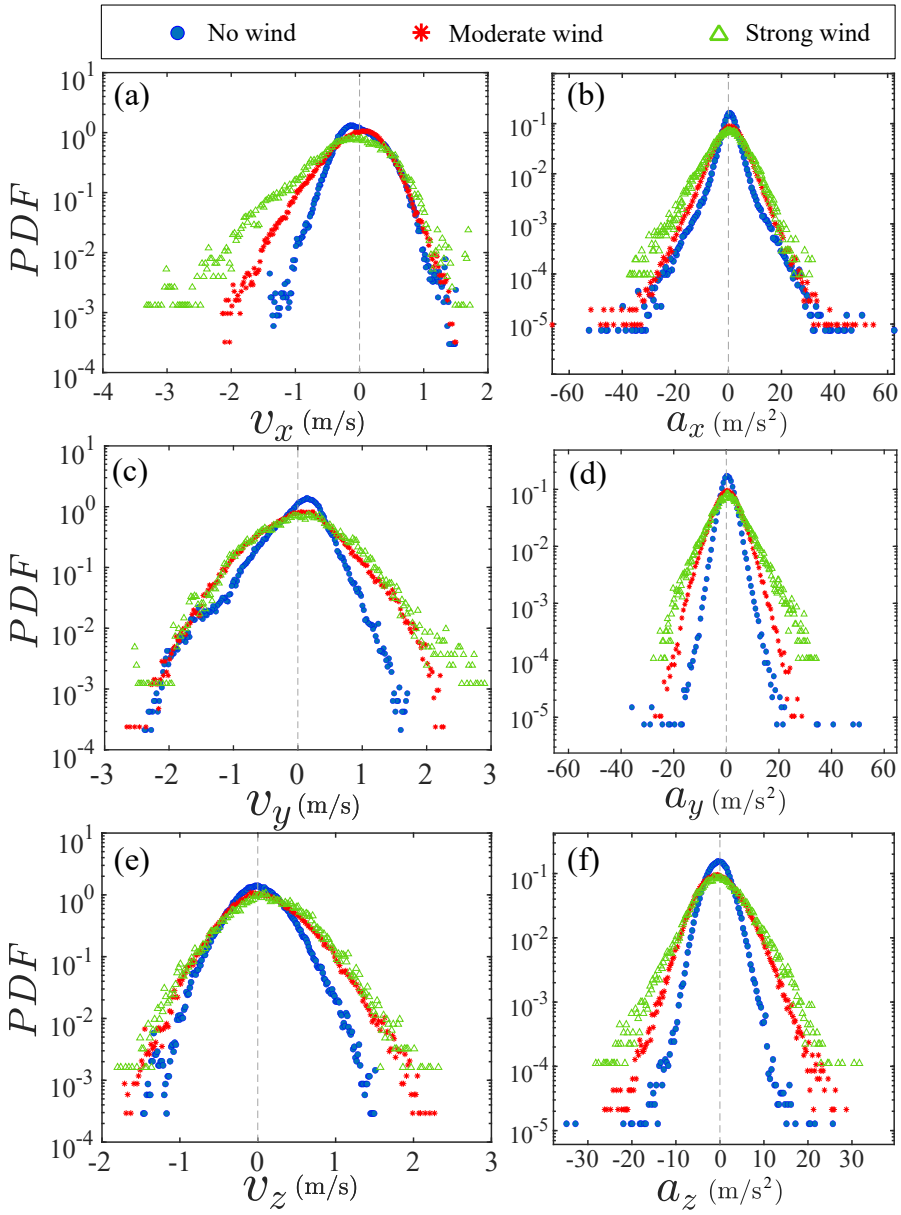

Figure 3. The probability distribution function (PDF) for honeybee velocity and acceleration components in different wind conditions. (a,b) x components, (c,d) y components, and (e,f) z components. The average velocity and accelerations increase with wind strength. The mean wind direction is in the $+y$, $-x$, and $+z$ direction.

velocity is skewed in the same direction as the mean wind velocity for all components of v. The acceleration components do not have a strong preferential direction but as the wind intensity increases, the mean acceleration magnitude also increases, this is also the case for the mean honeybee velocity magnitude. The mean honeybee velocity and acceleration magnitudes in different wind conditions are given in Table 3.

Figure 4 shows the PDF of the honeybee flight power per insect mass, defined as $P = a \cdot v$. We assume that the mass difference between honeybees is negligible as compared to to the variance in their velocity and acceleration. We calculate the

Table 3. The mean velocity, acceleration, and power magnitudes for each wind condition experiment.

Exp.	$\langle\lvert v\rvert\rangle$ (m/s)	$\langle\lvert a\rvert\rangle$ (m/s^2)	$\langle\lvert P\rvert\rangle$ (m^2/s^3)
No wind	0.53	4.52	1.17
Moderate wind	0.72	7.58	2.84
Strong wind	0.86	9.43	4.73

flight power using definitions from Lagrangian turbulence used to determine the change in kinematic energy of tracer particles advected in turbulent flow (Xu et al., 2014). Similarly to the mean velocity and acceleration magnitudes, the mean flight power magnitude also increases with increased wind velocity. In previous work we had observed that the mean flight performance of honeybees ($\langle\lvert v\rvert\rangle$, $\langle\lvert a\rvert\rangle$, and $\langle\lvert P\rvert\rangle$) did not change as we changed the wind turbulence intensity (Hejazi et al., 2022). In our previous experiments the mean wind velocity did not change significantly and was approximately uniform for all turbulence intensities investigated. However, now by significantly changing the mean wind velocity we clearly see a dependence of the flight performance on wind intensity.

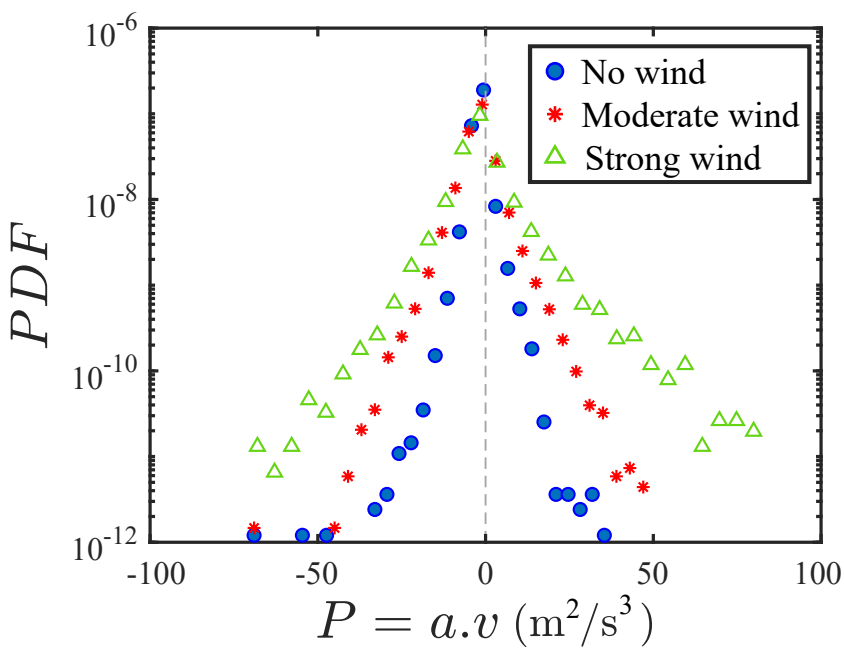

Figure 4. The PDF of honeybee flight power, $P = a \cdot v$, for different wind conditions. The average flight power is increasing with mean wind velocity.

Performing experiments in front of the hive entrance allowed us to also study the differences between landing and takeoff dynamics. For example, we showed that in no wind conditions (Fig. 3 (a)), honeybees have larger velocities when leaving the hive. The high-resolution images of our experiments allowed us to also determine the honeybee

body orientation. Fig. 5 (a-d) shows the raw images obtained with our four cameras at the same instance in time. The honeybee identified with the green square frame is seen on all four cameras at this frame. Fig. 5 (e-h) shows the zoomed in image of the honeybee identified in Fig. 5 (a-d). We calculated the honeybee orientation using a 3D capsule-like shape. The raw images were background subtracted and inverted resulting in a clear image intensity gradient from honeybee to background. The modeled shape was also given an intensity gradient similar to the actual image of the honeybee for improved optimization. The 3D model was then projected onto the four two-dimensional (2D) image planes and optimized so that the differences in pixel intensity between the actual honeybee image and projected model image was minimized. With this method we were able to find the honeybee orientation as shown in Fig. 5 (i-l), where the beginning and end of the projected model image are shown on the actual honeybee image. The honeybee center and reprojected center is also shown to demonstrate the tracking precision. The reprojected center was obtained by reprojecting the 3D steromatched point, obtained using the honeybee center initially found from the four camera images, back to the 2D camera image plane. Fig. 5 (m-p) show the optimized projection of the model capsule-like shape on the 2D camera image planes at the location of the honeybee identified in the previous figure panes.

Figure 6 shows the cosine of the angle between the honeybee body vector, $\hat{p}$, and the horizontal axis $\hat{y}$. The vector that defines the honeybee body orientation is the vector that lies along the length of the honeybee body from the tail to head or end to beginning of the honeybee as shown in Fig. 5 (i-l). In Fig. 6 (a), $\hat{p}\cdot\hat{y} < 0$ and the honeybee is facing away from the hive and is generally flying away from the hive. Similarly in Fig. 6 (b), $\hat{p}\cdot\hat{y} > 0$ and the honeybee is facing towards the hive and is generally flying towards the hive. The reason we use the term generally is that occasionally when the hive entrance was crowded the honeybees hovered or flew backwards away from the hive while facing towards the hive. It is worth noting that in no wind conditions (blue filled circles), we observed many more honeybees flying towards the hive than flying away from the hive, most likely due to the busy nature of the hive entrance and the need to find an opening to land. Additionally, it appears that the honeybees have a preferential body orientation while they fly away and towards the hive in no wind conditions, as can be seen by the maxima in the PDF of the cosines. In no wind conditions, the honeybees have larger angles away from the horizontal as they approach the hive in anticipation of landing as compared to when leaving the hive with larger velocities (Fig. 3 (c)). However, this preferential body angle while flying disappears when we introduce wind and the honeybees prefer to fly in a way that their body is mostly horizontal and aligned with $\hat{y}$. This more horizontal flight could perhaps be to increase flight stability in windy and unstable conditions.

We calculated the honeybee angular velocity from the honeybee body orientation. Fig. 7 shows the PDF of the honeybee angular velocity where $\omega_n = (1/3)(P(\omega_x/\omega'_x) + P(\omega_y/\omega'_y) + P(\omega_z/\omega'_z))$, and ω'_i is the standard deviation of ω_i. The angular velocity does not represent the complete angular dynamics of the honeybee since with our orientation

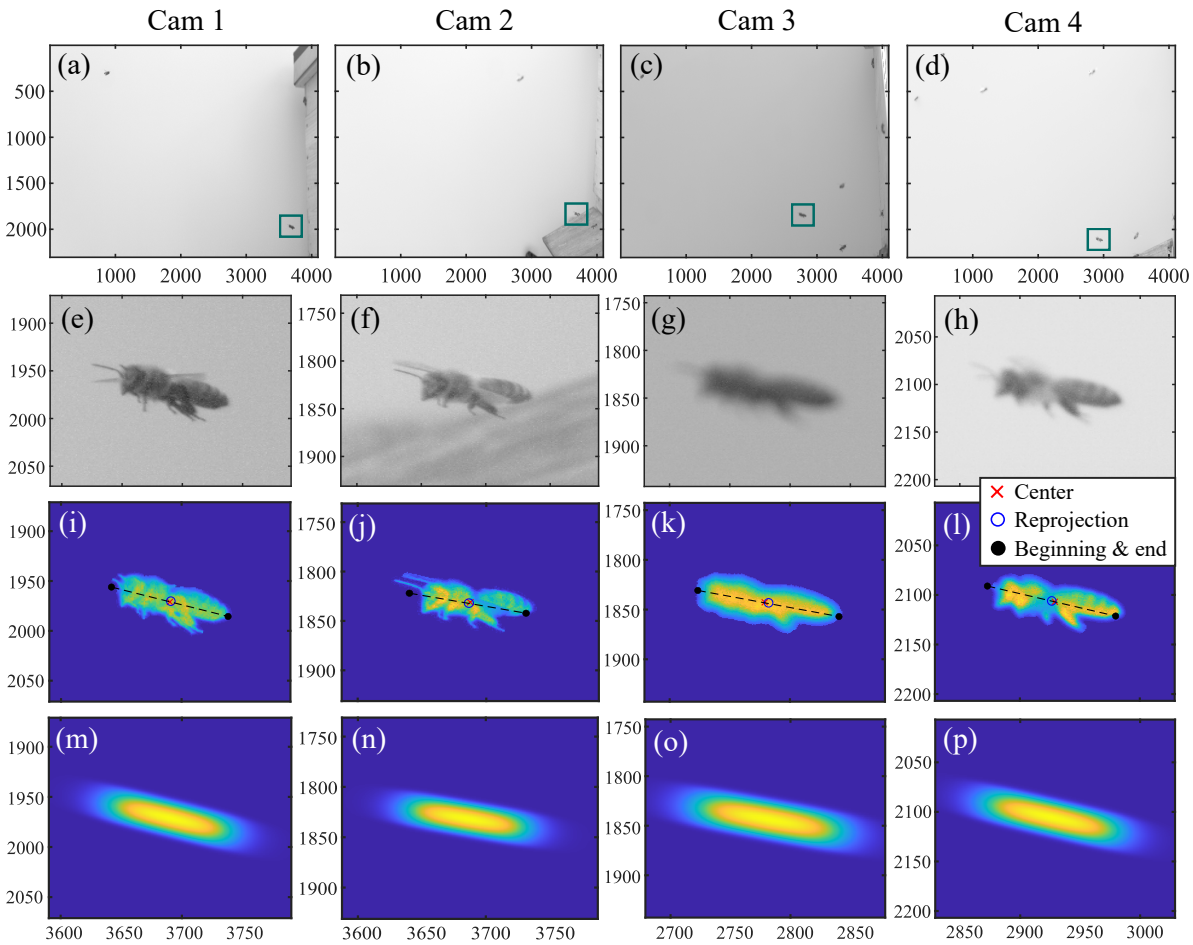

Figure 5. Example of honeybee orientation finding procedure. (a-d) raw images from the cameras at the same frame number where an identified honeybee is seen on all four cameras and is tracked. (e-h) Zoomed in image of the identified honeybee in (a-d). (i-l) Background subtracted and processed image of the honeybee where the center, beginning, and end of the honeybee are identified by fitting a capsule-like shape to the honeybee. (m-p) The capsule model that is fitted to the honeybee at the same position as the honeybee in (i-l).

finding method we can only obtain two of the three flight angles. The angular velocity shown in Fig. 7 represents the changes in the pitch and yaw of the honeybee and does not include roll dynamics. Even so, we can still observe interesting dynamics where just as before for the other flight parameters, the mean angular velocity increases with wind mean flow velocity. Table 4 shows the values for the mean angular velocity magnitudes for each wind condition experiment.

The major advantage of performing experiments in front of the hive entrance was that we were able to image multiple honeybees simultaneously. This allowed us to obtain pair statistics such as the PDF of the distance between every two honeybees seen at the same instance in time, Fig. 8 shows this PDF for all wind conditions. Amazingly the honeybees appear to be maintaining an optimal distance from one another independent

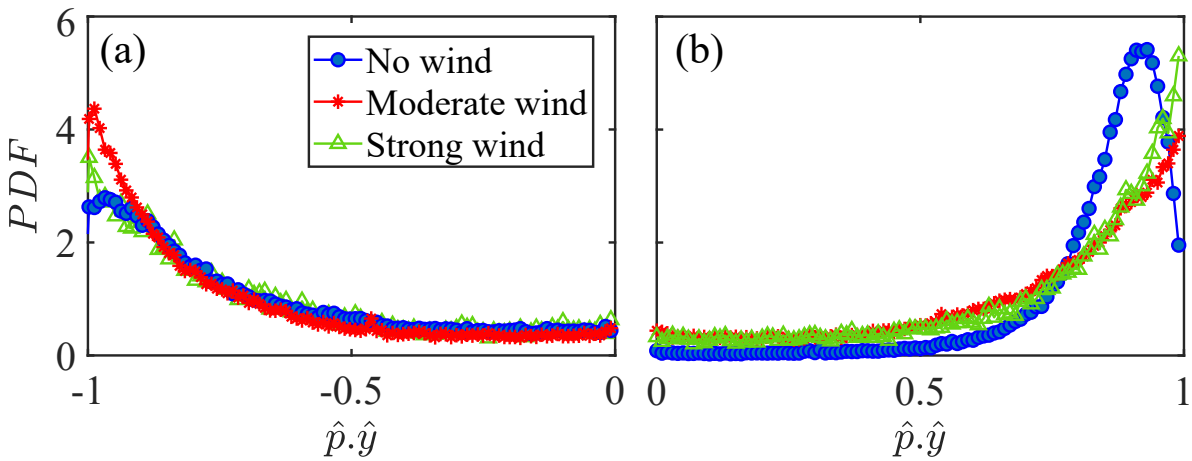

Figure 6. Cosine of the angle between the honeybee body vector, $\hat{p}$, and the global $\hat{y}$ vector for different wind conditions. (a) Honeybee is facing away from the hive and is generally moving away from the hive, (b) honeybee is facing towards the hive and is generally moving towards the hive.

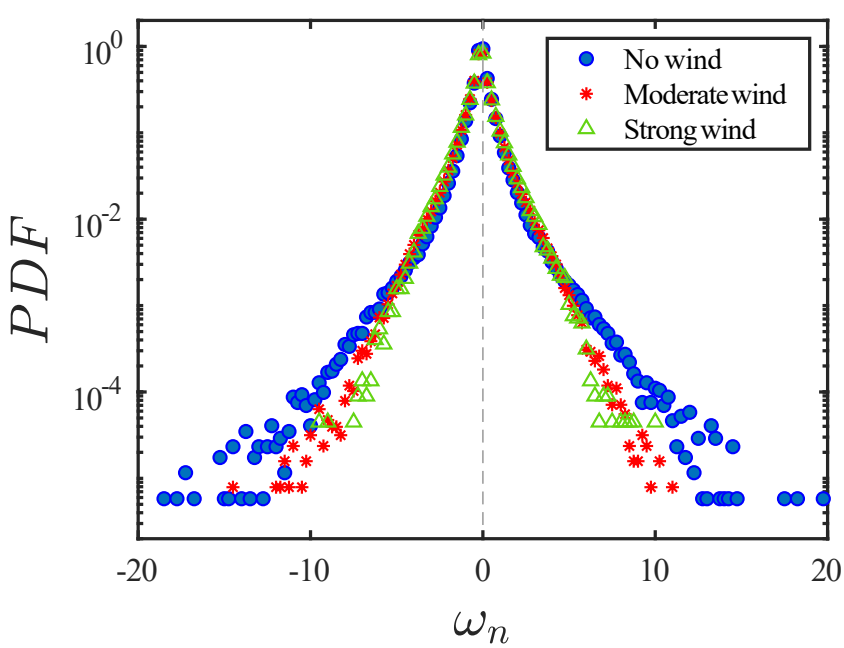

Figure 7. The PDF of honeybee angular velocity in different wind conditions. Here the angular velocity is calculated based on the pitch and yaw angles. The average of angular velocities increases with mean wind velocity.

Table 4. The mean angular velocity magnitudes for each wind condition experiment.

Exp.	$\langle\lvert\omega\rvert\rangle$ (rad/s)
No wind	4.49
Moderate wind	8.58
Strong wind	10.01

of the wind intensity. While the honeybees seemingly have less control in their flight in extreme conditions since all the other flight parameters (v, a, P, and ω) were affected by the change in wind intensity, they still maintain a chosen distance from each other. Also shown in Fig. 8 is a magnified section of the pair separation PDF's to show the similarity for different wind intensities.

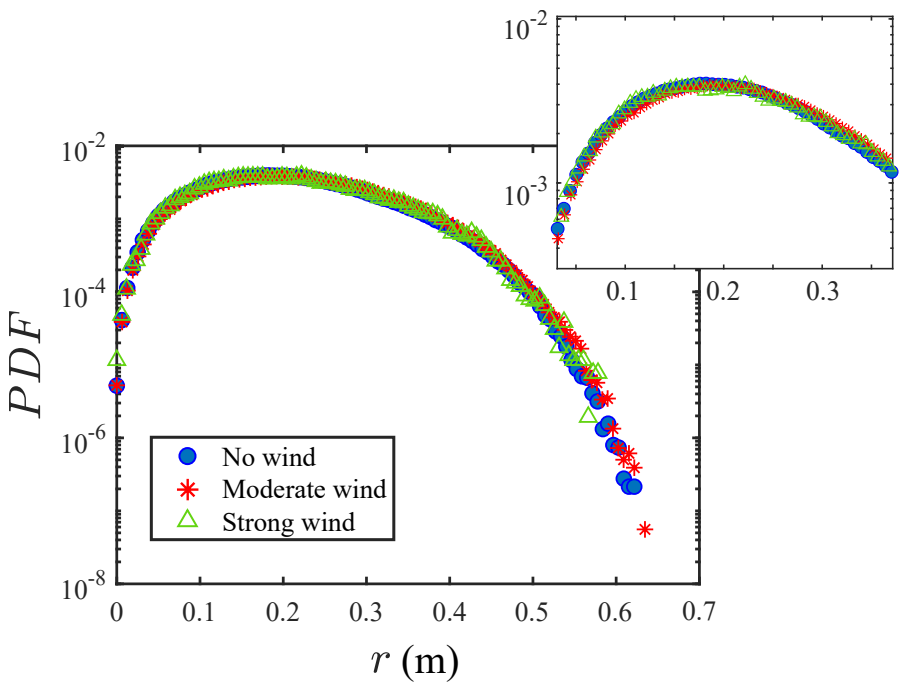

Figure 8. The PDF of the distance between every pair of honeybees seen at the same instance in time for different wind conditions. All wind conditions show the same behavior and the zoomed in section better demonstrates this.

4. Conclusions

The mean honeybee velocity, acceleration, flight power, and angular velocity were all influenced by the mean wind velocity where the mean magnitude of all the quantities measured increased with the mean wind velocity. In previous work we had observed at constant mean wind magnitudes that the measured quantities were not dependent on the turbulence intensities (Hejazi et al., 2022). Thus we conclude that it is the mean wind

and not the turbulence intensity to which the honey bees respond by changing these properties. In calm no wind conditions the honeybees have a preferential orientation in which they approach and leave the hive. The approach angle is larger than the leaving angle. With wind the honey bees align their bodies with the horizontal axis. Such behavior is perhaps a way to increase flight stability in windy conditions. The limitation to our orientation finding method is that we can only identify two of the three flight angles, namely we can only measure changes in the pitch and yaw. In future work we will also measure roll dynamics with the use of more advanced computer vision techniques (Mathis et al., 2018). By performing experiments in front of the hive entrance we explored the interaction between individual honeybees. We found that the honeybees maintain an optimal distance from one another during flight for all wind conditions. This distance was kept approximately constant even under extreme wind conditions while the honeybees had to adjust their flight parameters. Future work would need to explore this phenomena in more detail and explore under what conditions the pair separation between honeybees can be influenced. The results presented here on how honeybees fly in extreme winds and how their flight is affected, from their body orientation to their pair separation, can be of great interest to the advancement of flight stability, control, and the swarm intelligence needed for collision avoidance systems in robotics.

Acknowledgments

This work would not have been possible without the support of the technical staff at the MPI-DS. The authors would like to thank the biology staff for taking care of the honeybee hives. We would like to thank the experimental technicians for help with setting up the mobile laboratory and pavilion. Additionally, many thanks to the IT and HPC team for the setup of the data servers for file transfer and storage. We would like to express our sincere gratitude to Alain Pumir for insightful discussions.

Data and code availability

Available upon reasonable request.

Author contributions

BH planning and development of research project. BH, HA, and SH performing experiments and initial orientation analysis. BH analysis of data and writing original draft. BH, HA, SH, and EB editing and preparation of final draft.

Funding

We would like to thank the Max-Planck-Gesellschaft for support of this work.

Ethics statement

According to the representative for animal experiments in basic research at the Max Planck Society, no ethical or legal statements are required for the experiments presented in this work.

Competing interests

The authors declare no competing interests

References

I. Ahmed, C. I. Abramson, and I. A. Faruque. Honey bee flights near hover under ethanol-exposure show changes in body and wing kinematics. *PLOS ONE*, 17(12): 1–15, 12 2022. doi: 10.1371/journal.pone.0278916. URL `https://doi.org/10.1371/journal.pone.0278916`.

D. L. Altshuler, W. B. Dickson, J. T. Vance, S. P. Roberts, and M. H. Dickinson. Short-amplitude high-frequency wing strokes determine the aerodynamics of honeybee flight. *Proceedings of the National Academy of Sciences*, 102(50):18213–18218, 2005. doi:

10.1073/pnas.0506590102. URL https://www.pnas.org/doi/abs/10.1073/pnas.0506590102.

A. Attanasi, A. Cavagna, L. Del Castello, I. Giardina, S. Melillo, L. Parisi, O. Pohl, B. Rossaro, E. Shen, E. Silvestri, and M. Viale. Collective behaviour without collective order in wild swarms of midges. *PLOS Computational Biology*, 10(7):1–10, 07 2014. doi: 10.1371/journal.pcbi.1003697. URL https://doi.org/10.1371/journal.pcbi.1003697.

Z. Babic, R. Pilipovic, V. Risojevic, and G. Mirjanic. Pollen bearing honey bee detection in hive entrance video recorded by remote embedded system for pollination monitoring. *ISPRS Annals of the Photogrammetry, Remote Sensing and Spatial Information Sciences*, III-7:51–57, 2016. doi: 10.5194/isprs-annals-III-7-51-2016. URL https://www.isprs-ann-photogramm-remote-sens-spatial-inf-sci.net/III-7/51/2016/.

C. G. Butler and J. B. Free. The behaviour of worker honeybees at the hive entrance. *Behaviour*, 4(4):262–292, 1952. ISSN 00057959.

G. Chiron, P. Gomez-Krämer, and M. Ménard. Detecting and tracking honeybees in 3D at the beehive entrance using stereo vision. *EURASIP Journal on Image and Video Processing*, 2013, 2013. doi: 10.1186/1687-5281-2013-59. URL https://doi.org/10.1186/1687-5281-2013-59.

D. Clarke, H. Whitney, G. Sutton, and D. Robert. Detection and learning of floral electric fields by bumblebees. *Science*, 340(6128):66–69, 2013. doi: 10.1126/science.1230883. URL https://www.science.org/doi/abs/10.1126/science.1230883.

S. A. Combes and R. Dudley. Turbulence-driven instabilities limit insect flight performance. *Proceedings of the National Academy of Sciences*, 106(22):9105–9108, 2009. doi: 10.1073/pnas.0902186106. URL https://www.pnas.org/doi/abs/10.1073/pnas.0902186106.

J. D. Crall, J. J. Chang, R. L. Oppenheimer, and S. A. Combes. Foraging in an unsteady world: bumblebee flight performance in field-realistic turbulence. *Interface Focus*, 7(1):20160086, 2017. doi: 10.1098/rsfs.2016.0086. URL https://royalsocietypublishing.org/doi/abs/10.1098/rsfs.2016.0086.

K. S. Delaplane, D. R. Mayer, and D. F. Mayer. *Crop pollination by bees*. Cabi, 2000.

E. Farrell Helbling and R. J. Wood. A Review of Propulsion, Power, and Control Architectures for Insect-Scale Flapping-Wing Vehicles. *Applied Mechanics Reviews*, 70(1), 01 2018. ISSN 0003-6900. doi: 10.1115/1.4038795. URL https://doi.org/10.1115/1.4038795.

Y. Feng and N. T. Ouellette. Non-uniform spatial sampling by individuals in midge swarms. *Journal of The Royal Society Interface*, 20(199):20220521, 2023. doi: 10.1098/rsif.2022.0521. URL https://royalsocietypublishing.org/doi/abs/10.1098/rsif.2022.0521.

S. B. Fuller, A. D. Straw, M. Y. Peek, R. M. Murray, and M. H. Dickinson. Flying *Drosophila* stabilize their vision-based velocity controller by sensing wind with their antennae. *Proceedings of the National Academy of Sciences*, 111(13):E1182–E1191, 2014. doi: 10.1073/pnas.1323529111. URL `https://www.pnas.org/doi/abs/10.1073/pnas.1323529111`.

U. Greggers, G. Koch, V. Schmidt, A. Dürr, A. Floriou-Servou, D. Piepenbrock, M. C. Göpfert, and R. Menzel. Reception and learning of electric fields in bees. *Proceedings of the Royal Society B: Biological Sciences*, 280(1759):20130528, 2013. doi: 10.1098/rspb.2013.0528. URL `https://royalsocietypublishing.org/doi/abs/10.1098/rspb.2013.0528`.

J. Groening, L. McLeod, N. Liebsch, I. Schiffner, and M. V. Srinivasan. When left is right and right is wrong: Collision avoidance in honeybees. *Frontiers in Behavioral Neuroscience*, 235, 2012.

M. Harrington. Fruit flies in space. *Lab Animal*, 43(1):3–3, 2014. doi: 10.1038/laban.451. URL `https://doi.org/10.1038/laban.451`.

B. Hejazi. *Particle-Turbulence Interactions*. PhD thesis, Wesleyan University, 2021. URL `https://www.proquest.com/dissertations-theses/particle-turbulence-interactions/docview/2564145928/se-2?accountid=10474`.

B. Hejazi, M. Krellenstein, and G. A. Voth. Using deformable particles for single-particle measurements of velocity gradient tensors. *Experiments in Fluids*, 60(10), 2019. doi: 10.1007/s00348-019-2796-0. URL `https://doi.org/10.1007/s00348-019-2796-0`.

B. Hejazi, C. Küchler, G. Bagheri, and E. Bodenschatz. Honeybees modify flight trajectories in turbulent wind. *New Journal of Physics*, 24(11):113010, nov 2022. doi: 10.1088/1367-2630/ac9cc4. URL `https://dx.doi.org/10.1088/1367-2630/ac9cc4`.

K.-L. J. Hung, J. M. Kingston, M. Albrecht, D. A. Holway, and J. R. Kohn. The worldwide importance of honey bees as pollinators in natural habitats. *Proceedings of the Royal Society B: Biological Sciences*, 285(1870):20172140, 2018. doi: 10.1098/rspb.2017.2140.

E. R. Hunting, L. J. O'Reilly, R. G. Harrison, K. Manser, S. J. England, B. H. Harris, and D. Robert. Observed electric charge of insect swarms and their contribution to atmospheric electricity. *iScience*, 25(11), 2022. doi: 10.1016/j.isci.2022.105241. URL `https://doi.org/10.1016/j.isci.2022.105241`.

T. Jakobi, D. Kolomenskiy, T. Ikeda, S. Watkins, A. Fisher, H. Liu, and S. Ravi. Bees with attitude: the effects of directed gusts on flight trajectories. *Biology Open*, 7(10), 10 2018. ISSN 2046-6390. doi: 10.1242/bio.034074. URL `https://doi.org/10.1242/bio.034074`. bio034074.

B. Magnier, G. Ekszterowicz, J. Laurent, M. Rival, and F. Pfister. Bee hive traffic monitoring by tracking bee flight paths. In *13th International Joint Conference on*

Computer Vision, Imaging and Computer Graphics Theory and Applications, January 27-29, 2018, in Funchal, Madeira, Portugal, pages 563–571. Sept. 2018. doi: 10.5220/0006628205630571. URL https://hal.archives-ouvertes.fr/hal-01940300.

M. Y. Mahadeeswara and M. V. Srinivasan. Coordinated turning behaviour of loitering honeybees. *Scientific Reports*, 8(1), 2018. doi: 10.1038/s41598-018-35307-5. URL https://doi.org/10.1038/s41598-018-35307-5.

A. Mathis, P. Mamidanna, K. M. Cury, T. Abe, V. N. Murthy, M. W. Mathis, and M. Bethge. DeepLabCut: markerless pose estimation of user-defined body parts with deep learning. *Nature Neuroscience*, 21(9):1281–1289, 2018. doi: 10.1038/s41593-018-0209-y. URL https://doi.org/10.1038/s41593-018-0209-y.

T. N. Ngo, K.-C. Wu, E.-C. Yang, and T.-T. Lin. A real-time imaging system for multiple honey bee tracking and activity monitoring. *Computers and Electronics in Agriculture*, 163:104841, 2019. ISSN 0168-1699. doi: https://doi.org/10.1016/j.compag.2019.05.050. URL https://www.sciencedirect.com/science/article/pii/S0168169919301498.

V. M. Ortega-Jiménez and S. A. Combes. Living in a trash can: turbulent convective flows impair *Drosophila* flight performance. *Journal of The Royal Society Interface*, 15(147):20180636, 2018. doi: 10.1098/rsif.2018.0636. URL https://royalsocietypublishing.org/doi/abs/10.1098/rsif.2018.0636.

O. Peleg, J. M. Peters, M. K. Salcedo, and L. Mahadevan. Collective mechanical adaptation of honeybee swarms. *Nature Physics*, 14(12):1193–1198, 2018. doi: 10.1038/s41567-018-0262-1. URL https://doi.org/10.1038/s41567-018-0262-1.

O. Shishkov, C. Chen, C. A. Madonna, K. Jayaram, and O. Peleg. Strength-mass scaling law governs mass distribution inside honey bee swarms. *Scientific Reports*, 12(1), 2022. doi: 10.1038/s41598-022-21347-5. URL https://doi.org/10.1038/s41598-022-21347-5.

M. V. Srinivasan. Honeybees as a model for the study of visually guided flight, navigation, and biologically inspired robotics. *Physiological Reviews*, 91(2):413–460, 2011. doi: 10.1152/physrev.00005.2010. URL https://doi.org/10.1152/physrev.00005.2010.

M. Sun. Insect flight dynamics: Stability and control. *Review of Modern Physics*, 86: 615–646, May 2014. doi: 10.1103/RevModPhys.86.615. URL https://link.aps.org/doi/10.1103/RevModPhys.86.615.

G. P. Sutton, D. Clarke, E. L. Morley, and D. Robert. Mechanosensory hairs in bumblebees (¡i¿bombus terrestris¡/i¿) detect weak electric fields. *Proceedings of the National Academy of Sciences*, 113(26):7261–7265, 2016. doi: 10.1073/pnas.1601624113. URL https://www.pnas.org/doi/abs/10.1073/pnas.1601624113.

S. Vogel. Flight in Drosophila: I. Flight Performance of Tethered Flies. *Journal of Experimental Biology*, 44(3):567–578, 06 1966. ISSN 0022-0949. doi: 10.1242/jeb.44.3.567. URL https://doi.org/10.1242/jeb.44.3.567.

H. Xu, A. Pumir, G. Falkovich, E. Bodenschatz, M. Shats, H. Xia, N. Francois, and G. Boffetta. Flight-crash events in turbulence. *Proceedings of the National Academy of Sciences*, 111(21):7558–7563, 2014. doi: 10.1073/pnas.1321682111. URL `https://www.pnas.org/doi/abs/10.1073/pnas.1321682111`.

Z. Zeng, A. D. Ziegler, T. Searchinger, L. Yang, A. Chen, K. Ju, S. Piao, L. Z. X. Li, P. Ciais, D. Chen, J. Liu, C. Azorin-Molina, A. Chappell, D. Medvigy, and E. F. Wood. A reversal in global terrestrial stilling and its implications for wind energy production. *Nature Climate Change*, 9(12):979–985, 2019. doi: 10.1038/s41558-019-0622-6. URL `https://doi.org/10.1038/s41558-019-0622-6`.